1 **TITLE: Predicting *Vibrio cholerae* infection and disease severity using metagenomics in a**
2 **prospective cohort study**
3
4 **AUTHORS:** Inès Levade[1], Morteza M. Saber[1], Firas Midani[2,3,4], Fahima Chowdhury[5], Ashraful
5 I. Khan[5], Yasmin A. Begum[5], Edward T. Ryan[6,7,9], Lawrence David[2,3,4,8], Stephen B.
6 Calderwood[6,7,10], Jason B. Harris[6,11], Regina C. LaRocque[6], Firdausi Qadri[5], B. Jesse Shapiro[1*],
7 Ana A. Weil[12]
8
9 [1]Department of Biological Sciences, University of Montreal, Montreal, Quebec, Canada.
10 [2]Program in Computational Biology and Bioinformatics, Duke University, Durham, NC, USA
11 [3]Center for Genomic and Computational Biology, Duke University, Durham, NC, USA
12 [4]Department of Molecular Genetics and Microbiology, Duke University, Durham, NC, USA
13 [5]Center for Vaccine Sciences, International Centre for Diarrhoeal Disease Research, Dhaka,
14 Bangladesh
15 [6]Division of Infectious Diseases, Massachusetts General Hospital, Boston, MA, USA
16 [7]Department of Medicine, Harvard Medical School, Boston, MA USA
17 [8]Department of Biomedical Engineering, Duke University, Durham, NC, USA
18 [9]Department of Immunology and Infectious Diseases, Harvard T.H. Chan School of Public
19 Health, Boston, MA, USA
20 [10]Department of Microbiology, Harvard Medical School, Boston, MA USA
21 [11]Department of Pediatrics, Harvard Medical School, Boston, MA, USA
22 [12]Division of Allergy and Infectious Diseases, University of Washington, WA, USA
23

24 **CORRESPONDING AUTHOR** : jesse.shapiro@umontreal.ca

25

26 **RUNNING TITLE:** Stool metagenomics predicts cholera

ABSTRACT (word count: 196)

Background: Susceptibility to *Vibrio cholerae* infection is impacted by blood group, age, and pre-existing immunity, but these factors only partially explain who becomes infected. A recent study used 16S rRNA amplicon sequencing to quantify the composition of the gut microbiome and identify predictive biomarkers of infection with limited taxonomic resolution.

Methods: To achieve increased resolution of gut microbial factors associated with *V. cholerae* susceptibility and identify predictors of symptomatic disease, we applied deep shotgun metagenomic sequencing to a cohort of household contacts of patients with cholera.

Results: Using machine learning, we resolved species, strains, gene families, and cellular pathways in the microbiome at the time of exposure to *V. cholerae* to identify markers that predict infection and symptoms. Use of metagenomic features improved the precision and accuracy of prediction relative to 16S sequencing. We also predicted disease severity, although with greater uncertainty than our infection prediction. Species within the genera *Prevotella* and *Bifidobacterium* predicted protection from infection, and genes involved in iron metabolism also correlated with protection.

Conclusion: Our results highlight the power of metagenomics to predict disease outcomes and suggest specific species and genes for experimental testing to investigate mechanisms of microbiome-related protection from cholera.

KEYWORDS: *Vibrio cholerae,* cholera, microbiome, machine learning, metagenomics

MAIN TEXT (word count: 3407)

INTRODUCTION

Cholera is an acute diarrheal disease caused by *Vibrio cholerae*. Cholera is a major public health threat worldwide that continues to cause major outbreaks, such as in Yemen, where over 1.7 million cases have been reported since 2016 (1,2). Transmission of *V. cholerae* between household members commonly occurs through shared sources of contaminated food or water or through fecal-oral spread (3,4). The clinical spectrum of disease ranges from asymptomatic infection to severe watery diarrhea that can lead to fatal dehydration (5). Host factors such as age, innate immune factors, blood group, or prior acquired immunity partially explain why some people are more susceptible to *V. cholerae* infection than others, but a substantial amount of the variation remains unexplained (6).

The composition of the gut bacterial community can protect against enteropathogenic infections (7), and may explain some of the variation in *V. cholerae* susceptibility. Several studies have identified commensal bacteria and mechanisms that could be protective against *V. cholerae*. For instance, a species enriched in the gut microbiota of patients recovering from cholera, *Blautia obeum,* was found to interfere with *V. cholerae* pathogenicity through quorum-sensing inhibition in a mouse model (8). Animal and *in vitro* experiments have demonstrated that alteration of commensal-derived metabolite levels influenced host susceptibility by affecting *V. cholerae* growth or colonization (9-13).

Studies of *V. cholerae* and the gut microbiota often focus on a limited number of bacterial species or involve patients who already have symptomatic cholera (8,14). One study to date has characterized the gut microbiome of individuals exposed to *V. cholerae* to predict susceptibility to infection (15). In this study, Midani *et al*. developed a machine learning model to predict susceptibility based on 16S rRNA gene amplicon sequencing of the gut microbiota in a group of

76 household contacts of patients who have cholera, a group known to have high risk of infection
77 (4). Midani *et al* showed that the microbiome composition at the time of exposure to *V. cholerae*
78 can predict infection with similar or better accuracy as the commonly measured host factors
79 known to impact susceptibility. However, 16S rRNA sequencing does not allow identification of
80 precise strains or the underlying genetic factors of the observed relationship.

81 To increase our understanding of the relationship between the gut microbiome and
82 susceptibility to *V. cholerae*, we used shotgun metagenomics to analyze an expanded prospective
83 cohort of persons exposed to *V. cholerae* in Bangladesh. We sequenced all DNA obtained from
84 study participant rectal swabs (rather than only the 16S rRNA gene), and this resulted in
85 improved predictive power, including identification of specific genes associated with remaining
86 uninfected after exposure to *V. cholerae*. We also examined a larger cohort of samples to predict
87 disease severity among infected contacts, albeit with lower power and precision than our
88 susceptibility prediction. We also highlight several microbiome metabolic functions associated
89 with protection against cholera.

90 ## METHODS

91 **Sample collection, clinical outcomes and metagenomic sequencing**

92 As described in (15), household contacts were enrolled within 6 hours of the presentation
93 of an index cholera case at the icddr,b (International Center for Diarrheal Disease Research,
94 Bangladesh) Dhaka Hospital. Index patients with severe acute diarrhea, a stool culture positive
95 for *V. cholerae*, age between 2 and 60 years old, and no major comorbid conditions were
96 recruited (4,6). A clinical assessment of symptoms in household contacts was conducted daily for
97 the 10-day period after presentation of the index case, and repeated on day 30. We collected
98 demographic information, rectal swabs, and blood samples for ABO typing and vibriocidal
99 antibody titers as described in the Supplementary Methods. During the observation period,
100 contacts were determined to be infected if any rectal swab culture was positive for *V. cholerae*
101 and/or if the contact developed diarrhea and a 4-fold increase in vibriocidal titer during the
102 follow-up period (4,6). Contacts with positive rectal swabs developing watery diarrhea were
103 categorized as symptomatic and those without diarrhea were considered asymptomatic (**Figure**
104 **1**). *V. cholerae* positive contacts (by culture or 16S testing) at the time of enrollment were
105 excluded, in addition to contacts who reported antibiotic use or diarrhea during the week prior to
106 enrollment. DNA extraction was performed for the selected samples and used for shotgun
107 metagenomics sequencing. Detailed information on cohorts, sequencing methods and sample
108 processing are described in Supplemental Methods.

109

110 **Taxonomic/functional profiling and predictive model construction**

111 We used MetaPhlAn2 (version 2.9) (16) for taxonomic profiling and HUMAnN2 (17) was
112 used to profile cellular pathways (from MetaCyc) and gene families (identified using the PFAM
113 database of protein families). See the Supplementary Methods for further details on the

114 bioinformatic analyses. For identification of metagenomic biomarkers of susceptibility and
115 disease severity, we used MetAML (18), a computational tool for metagenomics-based prediction
116 tasks and for quantitative assessment of the strength of potential microbiome-phenotype
117 associations. We applied a random forests (RF) classifier on species, pathways and gene-family
118 relative abundances, as well as strain-specific markers presence/absence. Models constructed
119 using each of these different types of features were compared to each other, to a random dataset
120 with shuffled labels, and to a model constructed with clinical/demographic data, using two-
121 sample, two-sided *t*-tests over 20 replicate cross-validation, as previously described (18). We
122 used a stratified 3-fold cross validation approach, splitting our dataset into a validation set (1/3 of
123 samples) and a training set (2/3 of samples) with the same infected:uninfected ratio. The model
124 was first applied on all the features, then we used an embedded feature selection strategy to
125 identify the most useful features in the model and improve its accuracy. Feature relative
126 importance was computed using the mean decrease in impurity strategy, which calculates
127 importance of each feature as the sum of the number of nodes (across all trees) that use the
128 feature, proportional to the number of samples each of these nodes splits (18). Further details are
129 described in the Supplemental Methods.
130
131 **Data availability.**
132 After removal of human reads (Supplementary Methods), the sequence data has been
133 deposited in NCBI under BioProject PRJNA608678.
134

135 **RESULTS**

136

137 **Metagenomic sequencing of the gut microbiome in household contacts exposed to *V.***

138 ***cholerae***

139 We performed metagenomic sequencing of the gut microbiome in 65 contacts of cholera

140 cases from a cohort described by Midani *et al*. (15), from which sufficient DNA remained for

141 shotgun metagenomic sequencing. Of these 65 contacts, referred to as the Midani 2018 cohort, 20

142 developed infection during the follow-up period, and 45 remained uninfected (**Figure 1**). Among

143 the 20 contacts who became infected, 10 had no symptoms during the follow-up period (30 days),

144 and were classified as asymptomatic, and 10 developed symptoms (Supplementary Methods). To

145 increase our sample size, we surveyed an expanded cohort (**Table S1**) by adding 33 samples to

146 the Midani 2018 cohort, including 10 additional pre-infection samples from timepoints of

147 contacts in the Midani 2018 cohort, and 23 samples from 16 newly enrolled contacts from the

148 same population and the same time period (2012-2014, Dhaka, Bangladesh). We used pre-

149 infection samples in order to identify factors predictive of disease outcomes and identify

150 biomarkers in the microbiome of the Midani 2018 cohort, upon which we base the majority of

151 our analyses. We also performed exploratory analyses on the expanded cohort to determine the

152 potential for predictive models to be generalized to larger sample sizes.

153 We used the shotgun metagenomic DNA sequence reads from these samples to

154 characterize four features of the microbiome: 1) relative abundances of microbial species, 2) the

155 presence/absence of sub-species-level strains, 3) metabolic pathway relative abundances, and 4)

156 gene family relative abundances (**Table 1**).

157

158 **Predicting susceptibility to *V. cholerae* infection with Random Forest**

159 We first used an RF model to predict *V. cholerae* susceptibility (developing infection or
160 remaining uninfected) from baseline microbiome features (**Figure 1**). In the Midani 2018 cohort,
161 functional pathways and gene families predicted infection significantly better than random (Two-
162 sample *t*-tests comparing area under the curve [AUC] across 20 replicate 3 fold cross-validations;
163 $p < 0.05$) compared to data with shuffled (randomized) labels, and also predicted infection better
164 than species or strain features (**Table 1, Table S2**). Pathways and gene families had significantly
165 higher mean AUCs (0.71 and 0.74, respectively) compared to species or strains (0.61 and 0.62) (p
166 < 0.05; **Table 1**;**Figure S1, Table S3**).
167 To determine the minimum number of metagenomic features required for accurate
168 prediction, we repeated the analysis using smaller subsets of features. Using only 30 species, 60
169 gene families or pathways, or 200 strains achieved similar cross-validation AUC values (**Figure**
170 **S2**). We then trained an RF model on this reduced number of selected features, yielding improved
171 predictions for all feature types (**Figure S1; Table S4**). This suggests that only a limited number
172 of strains, species, genes and pathways in the gut microbiome at the time of exposure are
173 sufficient to predict *V. cholerae* susceptibility. For example, prediction using strain level markers
174 after feature selection yielded an AUC of 0.95 (**Table S4**). However, such high AUC values
175 should be treated with caution because the models can be overfit when a supervised feature
176 selection step is applied on the same data used to train the model (18). Because we did not have a
177 fully independent validation cohort (*e.g.* from another continent) to test our model, we decided to
178 use the features selected from the Midani cohort to make predictions on the Expanded dataset.
179 Using the same features selected from the Midani 2018 training dataset, we made predictions on
180 the Expanded cohort and achieved AUCs between 0.89 and 0.93 for prediction of infection using
181 the four types of features (**Table S4**). Again, because the expanded cohort partly overlaps with
182 the Midani cohort, and includes some repeated samples from the same individuals on different

183 study days, these results could also be prone to overfitting, but they demonstrate the potential for
184 generalized predictions.
185 Finally, we repeated the RF analysis using all features in the expanded dataset and found
186 that this increased predictive performance relative to the original Midani cohort (**Figure S1**).
187 Once again, genes and pathways outperformed species and strains according to all metrics, with
188 AUC reaching ~0.88 using cellular pathways (**Table 1**). This improvement in the expanded
189 cohort also highlights the importance of using larger and more balanced datasets as input to
190 predictive models.
191
192 **Improved prediction compared to known factors impacting susceptibility**
193 To put the metagenomic predictions in context, we next compared their predictive power
194 and accuracy to clinical and demographic factors (**Table S1**). Three of these factors (age,
195 baseline vibriocidal antibodies and blood group) are known to impact susceptibility to *V.*
196 *cholerae* infection (6,15) (**Table S5**). The likelihood of developing infection was not predicted
197 well using a RF model trained on the 7 features clinical and demographic factors (AUC=0.60, not
198 significantly different from shuffled labels, p=0.66; **Figure 2**). Predictions were not improved
199 using all species-level metagenomic features present at the time of exposure to *V. cholerae*
200 (AUC=0.61), but significantly improved using a selected number of species (AUC=0.80, $p < 1$
201 $\times 10^{-7}$). The use of all gene families or a selected number of genes showed an increased predictive
202 performance (AUC=0.74 and AUC=0.89 respectively; **Figure 2**) compared to species-level or
203 clinical and demographic contact data ($p < 1 \times 10^{-7}$ for all comparisons). We again note the caveat
204 that models with selected features may be overfit and represent an upper bound for predictive
205 power. Even without feature selection, we found that gene families clearly provide superior
206 predictions, and adding clinical data did not improve the predictions based on microbiome

207 features alone (**Figure 2**). Together, these results demonstrate that gene families present in the
208 gut microbiome at the time of exposure contain more information about *V. cholerae* susceptibility
209 compared to species-level or clinical and demographic contact data.
210

211 **Disease severity is more difficult to predict than likelihood of infection**

212 To predict symptomatic disease among infected individuals (**Figure 1**), we divided
213 samples into uninfected, symptomatic and asymptomatic groups and again applied the RF
214 approach. We used the F1 score as a performance metric since it is well suited for uneven class
215 distributions in our uninfected/symptomatic/asymptomatic comparison. Applied to the Midani
216 2018 cohort, this model predicted outcomes significantly better than random (shuffled labels)
217 using species, strains or pathway data, but not gene families (**Table 1;** see **Table S3** for *p*-
218 values). However, the F1 scores for the symptomatic/asymptomatic predictions were
219 systematically lower (mean scores ranging from of 0.57 to 0.60) than for the infected/uninfected
220 prediction (means ranging from 0.64 to 0.71). Using the expanded cohort, the scores were
221 improved only slightly (**Table 1**). These results suggest that disease severity is predictable in
222 principle, but with greater uncertainty than the simpler infection outcome.
223

224 **Taxonomic biomarkers of disease susceptibility and severity**

225 Predictive features in the gut microbiome identified to a species/strain or gene level allow
226 the possibility of experimental follow-up to investigate mechanisms of the associations we
227 observed. We characterized the most predictive species, pathways, and gene families (**Tables S6-**
228 **S9**). The most common discriminating species in individuals that remained uninfected during the
229 follow-up period were *Eubacterium rectale, Campylobacter hominis, Ruminococcus gnavus,*
230 *Bacteroides vulgatus, Veillonella parvula* and members of the *Prevotella* and *Eubacterium*

231 genera (**Figure 3A**, **Figure S3A and Figure S4A**). Several species associated with contacts that
232 developed *V. cholerae* infection belonged to the genera *Bifidobacterium, Actinomyces* or
233 *Collinsella*, and many of the species were also associated with asymptomatic infection (**Figure**
234 **3B**, **Figure S3B and Figure S4B**), including three species of *Bifidobacterium* (indicated with
235 asterisks in **Figure 3**). The top predictive species in contacts who developed symptomatic
236 infection were *Clostridium ventriculi* (formerly *Sarcina ventriculi*), *Streptococcus parasanguinis*
237 and members of the *Veillonella* genera. *Shigella* species were also associated with the gut
238 microbiome of persons who developed symptomatic *V. cholerae* infection, although persons
239 enrolled in this study were *Shigella* stool-culture negative. The features identified by the
240 multivariate RF model were confirmed using univariate statistics for the uninfected/infected
241 prediction (**Figure S5)**, but the overlap was poorer for the uninfected/symptomatic/asymptomatic
242 prediction (**Figure S6)**. This is consistent with the difficulty of correctly predicting disease
243 severity.
244
245 **Identification of functional biomarkers of disease susceptibility and severity**
246 We also identified gene families in the gut microbiome of persons who remained
247 uninfected during follow-up (**Figures S7 and S8)**, with some of the top gene families involved in
248 DNA repair, transmembrane transporter activity, iron metabolism (indicated with asterisks in
249 **Figure 4**), and genes of unknown function (**Table S8**). Long-chain fatty acid biosynthesis
250 pathways (*e.g.* cis-vaccenate, gondoate and stearate) were more likely to be associated with
251 individuals who remained uninfected, while amino acid biosynthesis pathways and catabolic
252 pathways were associated with individuals who developed infection (**Figures S9 and S10, Table**
253 **S9**). We identified three iron-related genes associated with individuals that remained uninfected:
254 (1) the ferric uptake regulator Fur, a major regulator of iron homeostasis, (2) thioredoxin, a redox

255 protein involved in adaptation to oxidative and iron-deficiency stress, and (3) the
256 TonB/ExbD/TolQR system, a ferric chelate transporter (19-21). In individuals who became
257 infected and were asymptomatic, two genes involved in the conversion of riboflavin into
258 catalytically active cofactors, the riboflavin kinase and the FAD synthetase, were found as the
259 first and the third most discriminant features (**Figure 4, Table S8**).
260 We next asked which taxa in the microbiome likely encoded these genes. In some cases,
261 specific taxonomic groups corresponded to discrete gene functions; for example, the *Prevotella*
262 genus was the major contributor to several iron metabolism related gene families (**Figure S12**).
263 In other cases, the major contributors to protective gene families were unclassified (**Figure 5 and**
264 **Figure S11**). These results partly explain why gene families or pathway features tend to
265 outperform species-level features in predicting infection status – because predictive gene families
266 are distributed across many species, including several with poor taxonomic annotation or families
267 lacking representation in taxonomic databases.
268

269 **DISCUSSION**

270 Cholera continues to cause widespread disease in populations without access to safe
271 water. The gut microbiome is a potentially modifiable host risk factor for cholera, and
272 identification of specific genes and strains correlated with susceptibility is needed for
273 experimental testing to understand the mechanisms of observed correlations. Compared to a
274 previous study using a single marker gene, shotgun metagenomics provides this degree of
275 resolution, potentially to the species and strain level, and to the level of individual genes and
276 cellular functions. We found that gene families in the gut microbiome at the time of exposure to
277 *V. cholerae* were more predictive of susceptibility compared to taxonomic or clinical and
278 demographic information.

279 Using a machine learning method to identify the most important factors contributing to
280 our model, we selected 30 bacterial species from 65 samples to estimate which contacts became
281 infected, and predicted outcomes with similar success rates as previously reported with 16S data
282 **(**15). Prediction of infection was substantially improved by using gene families or metabolic
283 pathways, highlighting the benefits of using richer metagenomic data. Selecting a subset of the
284 most informative features further improved predictions, but using these selected features may
285 lead to overfitting. This suggests an upper limit to predictive power that requires validation in
286 larger, independent cohorts.

287 Most of the top predictive biomarkers (using both species and gene families) were
288 associated with remaining uninfected after exposure to *V. cholerae*, and many of these
289 biomarkers were consistently identified (**Figures 3** and **4**). An example is the genus *Prevotella,*
290 including several strains within *Prevotella* sp. 885, identified only at the genus level in a previous
291 study(15). *Prevotella* species are hypothesized to be beneficial members of the microbiota in

292 healthy individuals in non-Westernized countries, and this species is a potential candidate for
293 follow up experimental studies in *V. cholerae* susceptibility (14,22,23).
294 Several species known to ferment mucin glycans into short chain fatty acids (SCFAs)
295 correlated with remaining uninfected, including *Eubacterium rectale*, *Ruminococcus gnavus* and
296 *Bacteroides vulgatu*s (24,25). This finding is consistent with experiments of SCFAs applied to
297 animal models. *B. vulgatus* has been shown to inhibit *V. cholerae* colonization in mice, an effect
298 that was dependent upon SCFAs butyrate and propionate production (13). SCFAs are known to
299 impact immune cell development and attenuate inflammation by inhibiting histone deacetylases
300 and other mechanisms of altering gene expression (26-29).
301 All three *Bifidobacterium* species associated with contacts that developed infection were
302 also associated with asymptomatic rather than symptomatic disease (**Figure 3**), and prior work on
303 this genera supports several hypotheses for this relationship. First, *Bifidobacteria* are known to
304 produce the SCFA acetate that can protect against enteric infection in mice (33,34)(30). SCFAs
305 are also known to inhibit cholera toxin-related chloride secretion in the mouse gut, reducing
306 water and sodium loss, and have also been observed to increase cholera toxin-specific antibody
307 responses (31-33). *Bifidobacteria* are also major producers of lactate, a metabolite that has been
308 shown to impair *V. cholerae* biofilm formation, a function that can impact pathogen virulence
309 (12). Lastly, *B. bifidum* and *B. adolescentis* are known to reduce the activity of the *V. cholerae*
310 type VI secretion system through modification of bile acids (9).
311 The use of metagenomics also allowed us to identify bacterial functions that could impact
312 the ability of *V. cholerae* to compete and colonize the gut. For example, several gene families
313 involved in iron transport, iron regulation, and riboflavin conversion appeared among the top
314 twenty features associated with uninfected and asymptomatic individuals, suggesting that
315 competition for iron might be a protective mechanism of the gut microbiota against *V. cholerae*,

316 as is the case for other pathogens (7). Iron is often a limiting redox cofactor in the gut, and
317 bacteria have evolved strategies to solubilize and internalize iron (34,35). Riboflavin (another
318 major redox cofactor in bacteria) and iron levels are reciprocally regulated in *V. cholerae*, and
319 more generally, riboflavin may allow *V. cholerae* to overcome iron limitation in the gut (34,36).
320 A gut microbiota more competitive for iron could be an important factor in resistance to *V.*
321 *cholerae* colonization or virulence. Further work is thus needed to understand mechanisms of
322 how the enrichment of these microbiome genes may protect people after exposure to *V. cholerae*.
323 Our results are currently not generalizable beyond the study cohort in Dhaka, Bangladesh,
324 since a similar cohort in another geographic location is not available. As with any association-
325 based study (37), it is unknown if any of the metagenomic features that correlate with protection
326 from *V. cholerae* infection are causal, and many may be markers of clinical or environmental
327 factors that themselves impact susceptibility. Further experimental characterization of
328 metagenomic features correlated with protection from infection or symptoms are needed to
329 understand if factors we identified impact *V. cholerae* pathogenesis or host responses to infection.
330 Ultimately, the strains and functionalities identified have the potential to inform microbiota-based
331 therapeutics to ameliorate or prevent disease. Our results show the power of metagenomic data
332 from the gut microbiome to predict health outcomes such as susceptibility to infection and
333 disease severity.

FUNDING INFORMATION

This study was supported by CIHR (Canadian Institutes of Health Research) and the Canada Research Chairs program (BJS), The icddr,b: Centre for Health and Population Research, the Alfred P. Sloan Fellowship (LAD), grants AI099243 (J.B.H and L.C.I), AI103055 (J.B.H and F.Q), AI106878 (E.T.R and F.Q.), AI058935 (E.T.R, S.B.C and F.Q.), T32A1070611976 and K08AI123494 (A.A.W.) from the National Institutes of Health, and the Robert Wood Johnson Foundation Harold Amos Medical Faculty Development Program (R.C.C.).

ACKNOWLEDGEMENTS

We thank Meti Debela for technical assistance. Finally, we are grateful to the people of Dhaka where our study was undertaken; to the field, laboratory and data management staff who provided tremendous effort to make the study successful; and to the people who provided valuable support in our study. The icddr,b gratefully acknowledges the Government of the People's Republic of Bangladesh; Global Affairs Canada (GAC); Swedish International Development Cooperation Agency (Sida) and the Department for International Development, (UKAid). We declare that we have no competing financial interest.

ETHICAL STATEMENT

The Ethical and Research Review Committees of the icddr,b and the Institutional Review Board of MGH reviewed the study. All adult subjects provided informed consent and parents/guardians of children provided informed consent. Informed consent was written.

CONFLICTS OF INTEREST

The authors declare that there are no conflicts of interest.

360 **FIGURES AND TABLES**

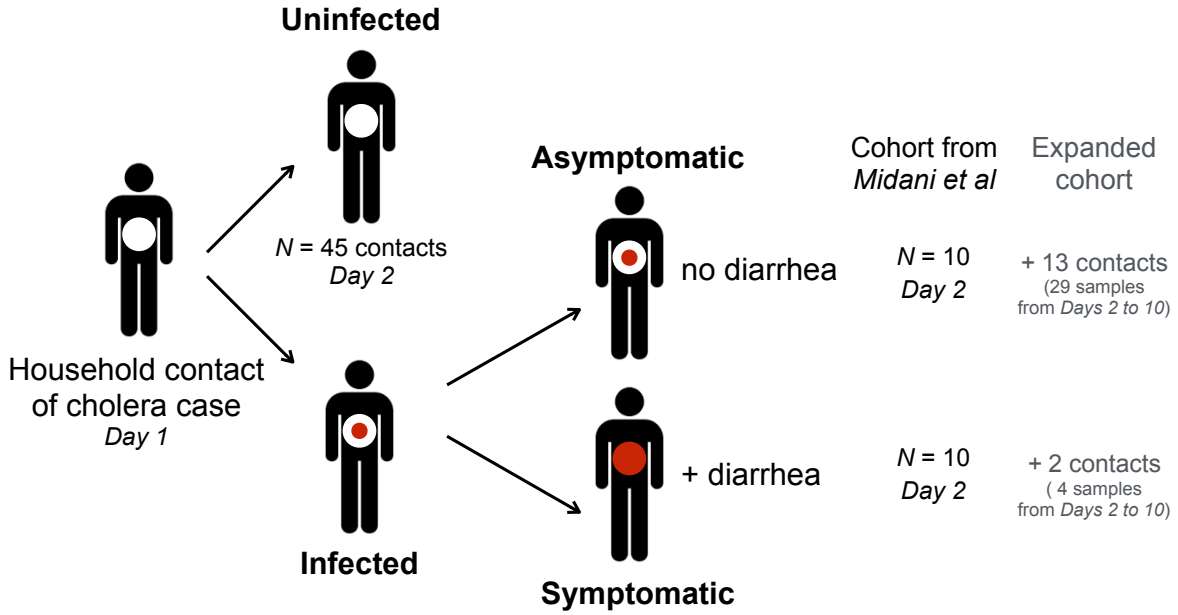

361
362 **Figure 1. Study cohort in Dhaka, Bangladesh.** After presentation of a *V. cholerae* culture-
363 positive index case to the hospital on day 1, household contacts were enrolled on day 2. The
364 expanded cohort includes the Midani 2018 cohort (15), with an addition of 33 samples from
365 infected individuals (13 asymptomatic and 2 symptomatic).

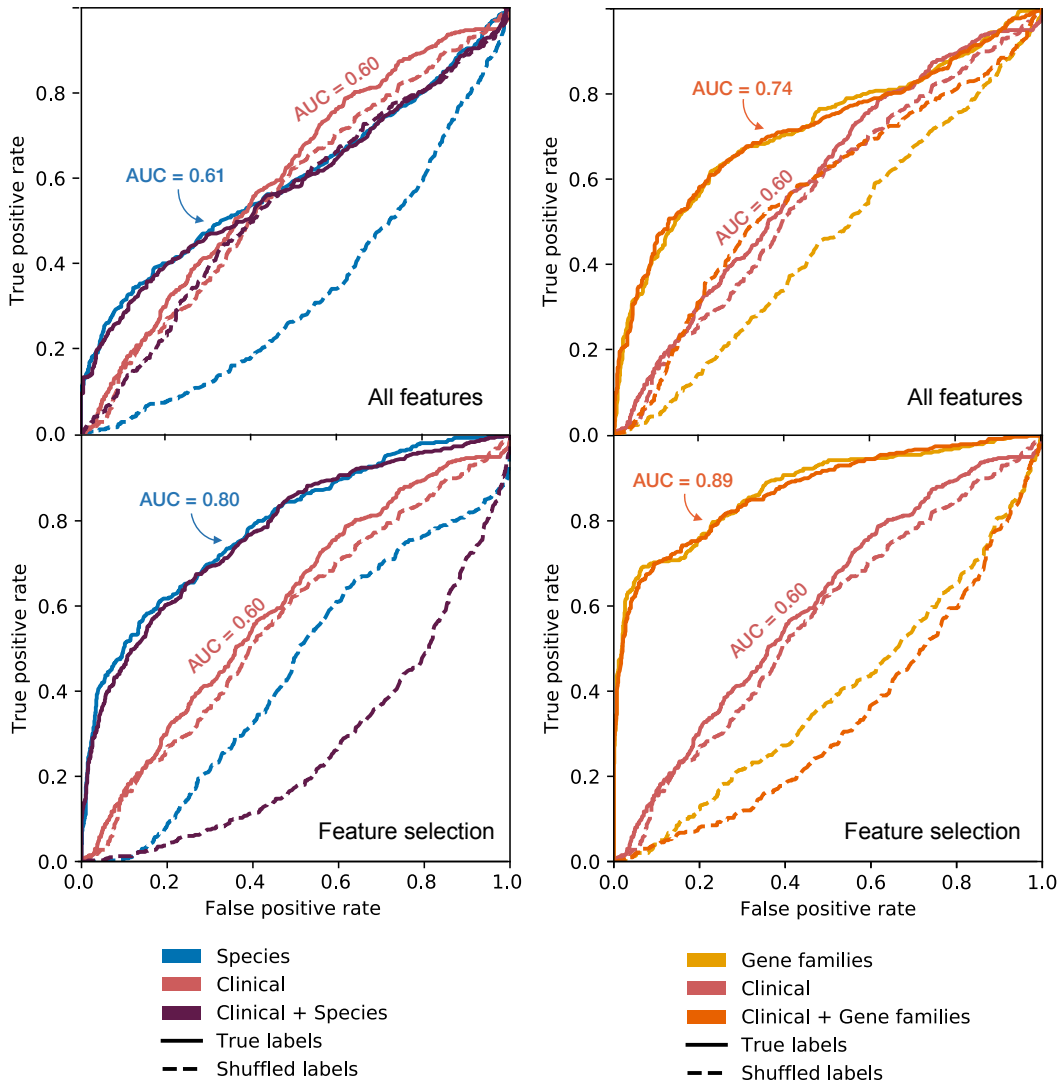

366 **Figure 2. Metagenomic features predict *V. cholerae* infection better than clinical and**
367 **demographic features.** Random forest prediction of infection status was applied to 7 clinical and
368 demographic features, and compared with all species and all gene families (top row), as well as
369 30 selected species features from metagenomes and 60 selected gene family features (bottom
370 row), or a combination of clinical, demographic and metagenomic features. Plots show receiver
371 operating characteristic (ROC) curves (average across cross-validations) for the Midani 2018
372 dataset. Shuffled labels represent the prediction run on a dataset with a random assignment of
373 infection outcomes. AUC = area under the curve.

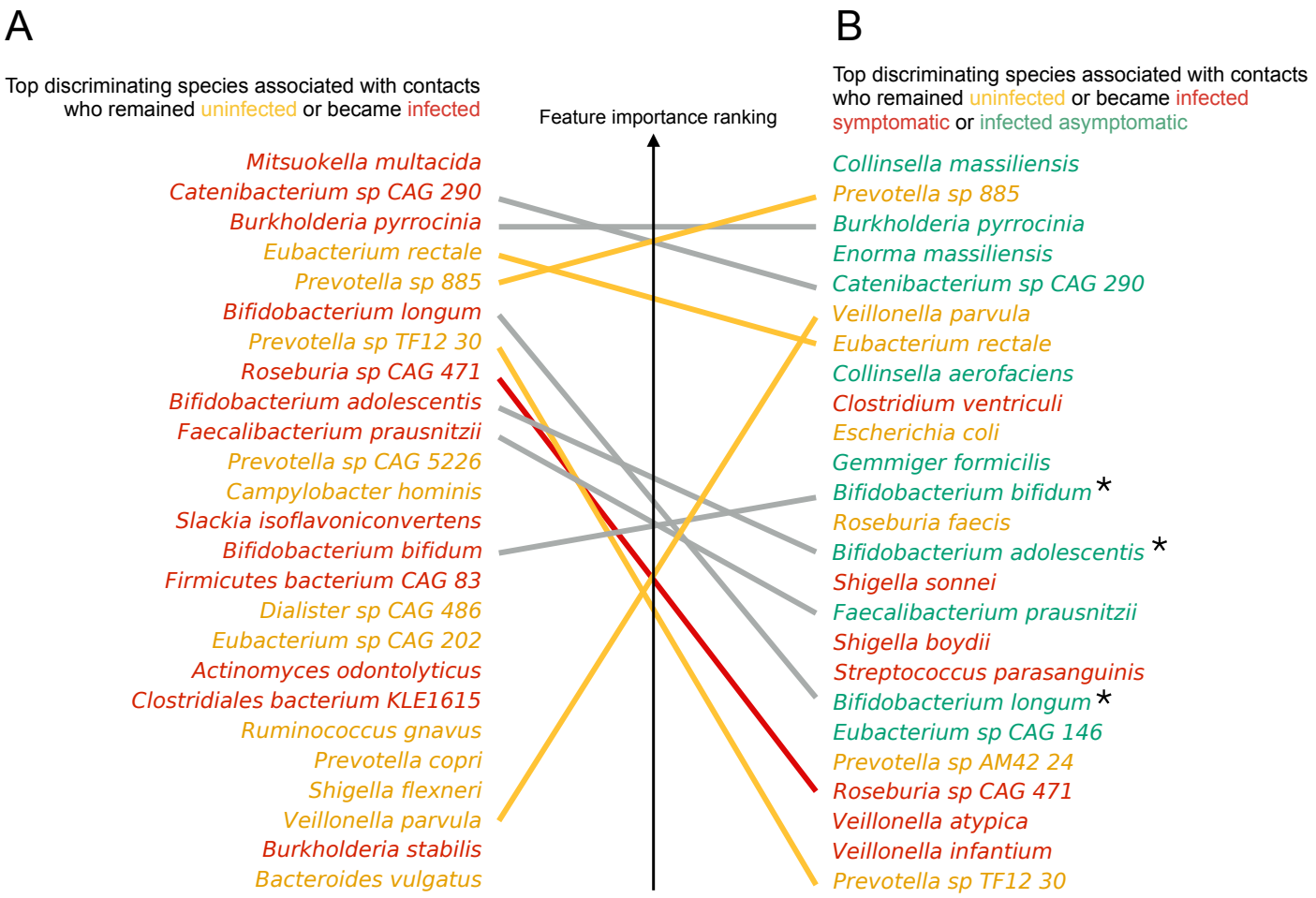

Figure 3. Most important discriminating species of the gut microbiome at the time of exposure to *V. cholerae* identified in the Midani 2018 dataset, classified by clinical outcome. (A) Species associated with contacts that became infected (red) or remained uninfected (yellow) during follow-up. (B) Species associated with contacts who remained uninfected (yellow), or became infected asymptomatic (green), or symptomatic (red) during follow-up. The top 25 most important features are shown here; see Table S6 for the full list. Yellow lines connect species associated with uninfected individuals in both (A) and (B); red lines connect species associated with infection in (A) and symptomatic disease in (B); grey lines connect species associated with infection in (A) but asymptomatic infection in (B). Three species of *Bifidobacterium* are marked with an asterisk.

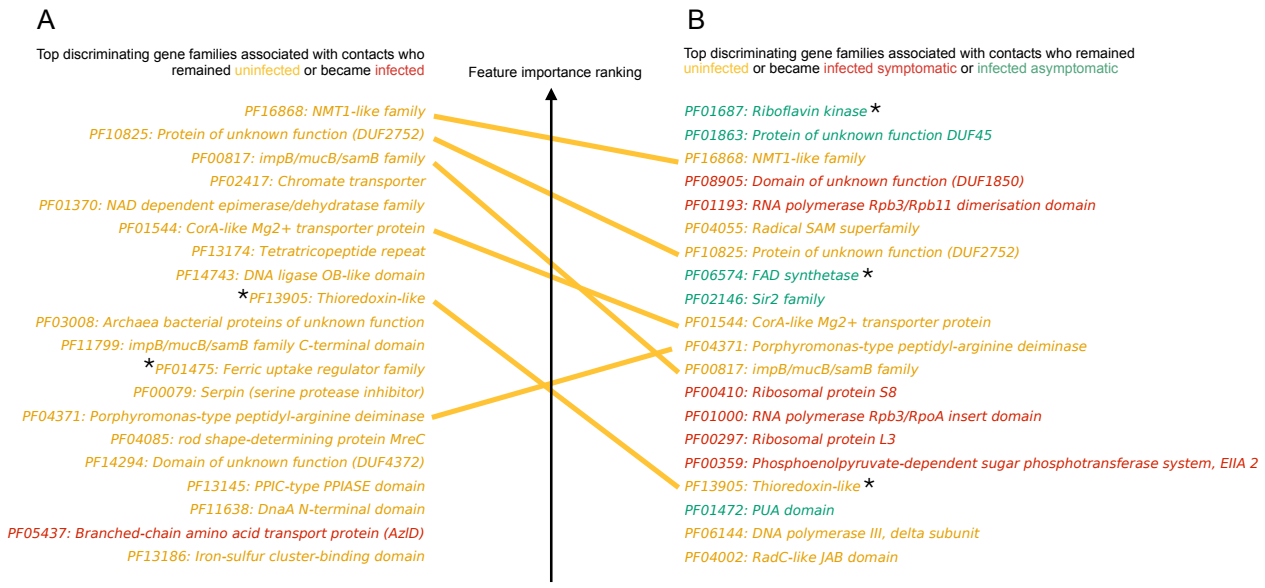

Figure 4. Most important discriminating gene families of the gut microbiome at the time of exposure to *V. cholerae* identified in the Midani 2018 dataset, classified by clinical outcome. (A) Genes families associated with contacts that became infected (red) or remained uninfected (yellow) during follow-up. (B) Genes families associated with contacts who remained uninfected (yellow), or became infected asymptomatic (green), or symptomatic (red) during follow-up. The top 25 most important features are shown here; see Table S8 for the full list. Yellow lines connect species associated with uninfected individuals in both (A) and (B). Asterisks indicate genes involved in redox or iron metabolism.

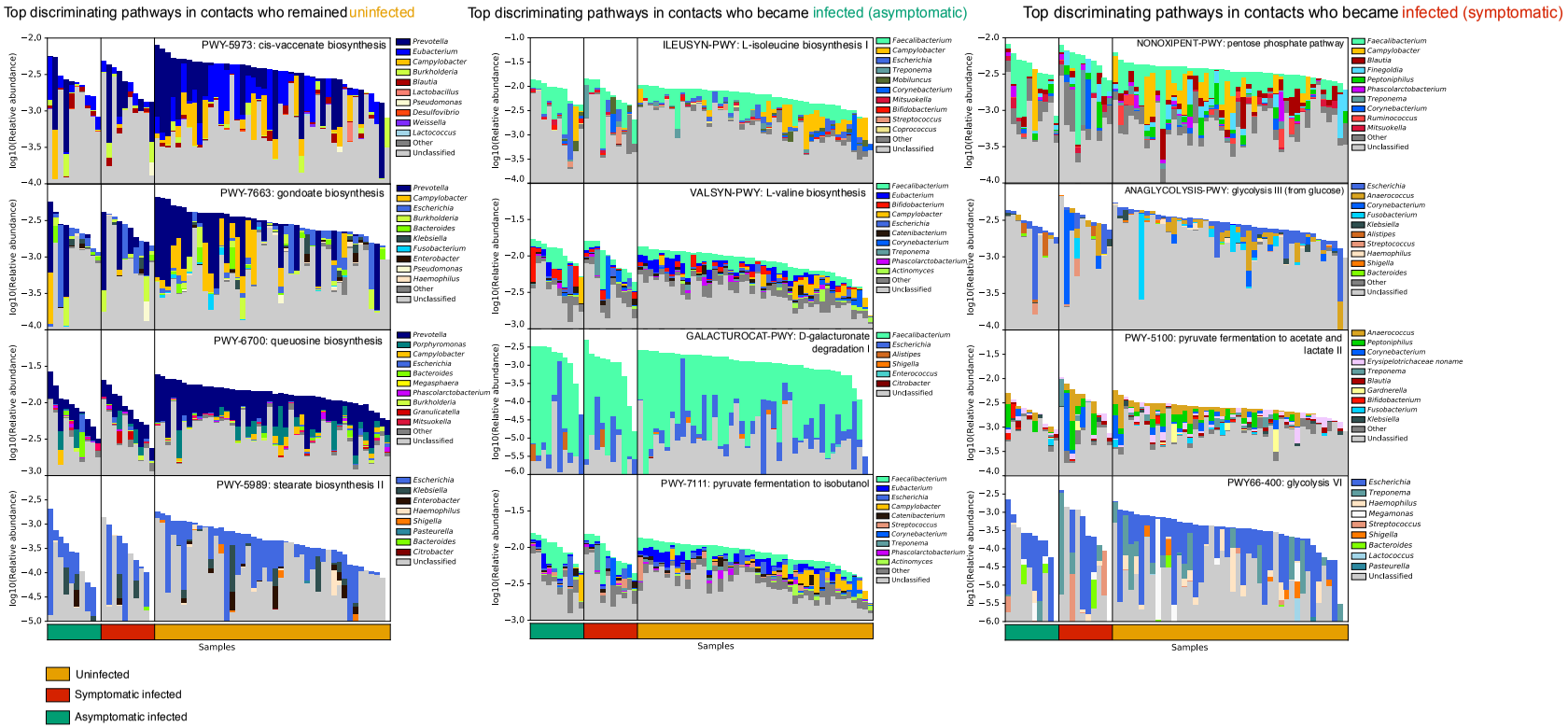

Figure 5. Top predictive cellular pathways of the gut microbiome at the time of exposure to *V. cholerae* in the Midani 2018 cohort, annotated by their taxonomic contributors. The four top-ranked pathways associated with uninfected contacts (left column), contacts who developed asymptomatic infection (middle), and contacts who developed symptomatic infection (right column) are shown. Total bar height reflects $\log_{10}$-scaled community relative abundance of each pathways. The contributions of each genus to encoding these pathways are shown as stacked colors within each bar, linearly scaled within the total. See Table S9 for the complete list of pathways.

402 **Tables**

403

		RF – Cohort from Midani et al				RF – Expanded			
		Species abundance	Strain markers	Gene families	Pathways	Species abundance	Strain markers	Gene families	Pathways
	#features	705	54953	6810	443	807	62965	7514	461
Infected Vs Uninfected	Accuracy	0.73 (±0.02)	0.71 (±0.02)	0.76 (±0.02)	0.72 (±0.02)	0.76 (±0.03)	0.69 (±0.03)	0.80 (±0.02)	0.80 (±0.03)
	Precision	0.71 (±0.06)	0.68 (±0.06)	0.77 (±0.04)	0.70 (±0.05)	0.76 (±0.03)	0.70 (±0.03)	0.81 (±0.02)	0.81 (±0.03)
	F1	0.66 (±0.02)	0.64 (±0.03)	0.71 (±0.03)	0.66 (±0.03)	0. 75 (±0.03)	0.68 (±0.03)	0.80 (±0.02)	0.80 (±0.03)
	AUC	0.61 (±0.05)	0.62 (±0.04)	0.74 (±0.04)	0.71 (±0.04)	0.83 (±0.02)	0.76 (±0.03)	0.87 (±0.02)	0.88 (±0.02)
Shuffled	F1	0.55 (±0.04)	0.56 (±0.04)	0.56 (±0.04)	0.56 (±0.05)	0.40 (±0.03)	0.45 (±0.03)	0.48 (±0.03)	0.44 (±0.03)
	AUC	0.40 (±0.04)	0.57 (±0.04)	0.50 (±0.05)	0.50 (±0.04)	0.39 (±0.03)	0.52 (±0.03)	0.51 (±0.03)	0.46 (±0.03)
Asymptomatic vs Symptomatic vs Uninfected	Accuracy	0.70 (±0.02)	0.70 (±0.02)	0.69 (±0.01)	0.69 (±0.01)	0.68 (±0.01)	0.60 (±0.03)	0.69 (±0.02)	0.67 (±0.03)
	Precision	0.53 (±0.03)	0.53 (±0.03)	0.60 (±0.02)	0.59 (±0.02)	0.60 (±0.02)	0.53 (±0.03)	0.61 (±0.02)	0.59 (±0.02)
	F1	0.60 (±0.02)	0.59 (±0.02)	0.57 (±0.02)	0.57 (±0.02)	0.62 (±0.02)	0.55 (±0.03)	0.64 (±0.02)	0.62 (±0.02)
	AUC	NA	NA	NA	NA	NA	NA	NA	NA
Shuffled	F1	0.48 (±0.04)	0.49 (±0.04)	0.46 (±0.03)	0.55 (±0.03)	0.41 (±0.03)	0.35 (±0.03)	0.44 (±0.04)	0.37 (±0.03)
	AUC	NA	NA	NA	NA	NA	NA	NA	NA

404

405 **Table 1. Assessment of prediction performance for a random forest (RF) model applied to**
406 **the Midani 2018 and expanded cohorts.** Species abundances, strain-specific markers
407 presence/absence, relative abundance of Pfam-grouped gene families, and MetaCyc pathways
408 were used as features. For each dataset, we applied a binary (uninfected vs. infected contacts) and
409 a multi-class (asymptomatic vs. symptomatic vs. uninfected contacts) classifier and reported
410 performance metrics for each dataset. Metrics obtained by the same classifier applied to the same
411 datasets with shuffled class labels (random assignment of labels to samples) are also reported
412 (shuffled). The margins of errors (95% confidence intervals) are reported in parenthesis.

413 **REFERENCES**
414

415 1. Ali M, Nelson AR, Lopez AL, Sack DA. Updated Global Burden of Cholera in Endemic
416 Countries. PLoS Negl Trop Dis. **2015**; 9(6):e0003832.

417 2. Camacho A, Bouhenia M, Alyusfi R, et al. Cholera epidemic in Yemen, 2016-18: an
418 analysis of surveillance data. Lancet Glob Health. **2018**; 6(6):e680–e690.

419 3. Domman D, Chowdhury F, Khan AI, et al. Defining endemic cholera at three levels of
420 spatiotemporal resolution within Bangladesh. Nat Genet. **2018**; :1–10.

421 4. Weil AA, Khan AI, Chowdhury F, et al. Clinical Outcomes in Household Contacts of
422 Patients with Cholera in Bangladesh. Clin Infect Dis. **2009**; 49(10):1473–1479.

423 5. Nelson EJ, Harris JB, Morris JG, Calderwood SB, Camilli A. Cholera transmission: the
424 host, pathogen and bacteriophage dynamic. Nature. **2009**; :1–10.

425 6. Harris JB, LaRocque RC, Chowdhury F, et al. Susceptibility to *Vibrio cholerae* Infection
426 in a Cohort of Household Contacts of Patients with Cholera in Bangladesh. PLoS Negl
427 Trop Dis. **2008**; 2(4):e221–8.

428 7. Ubeda C, Djukovic A, Isaac S. Roles of the intestinal microbiota in pathogen protection.
429 Clinical & Translational Immunology. **2017**; 6(2).

430 8. Hsiao A, Ahmed AMS, Subramanian S, et al. Members of the human gut microbiota
431 involved in recovery from *Vibrio cholerae* infection. Nature. **2014**; 515(7527):423–426.

432 9. Bachmann V, Kostiuk B, Unterweger D, Diaz-Satizabal L, Ogg S, Pukatzki S. Bile Salts
433 Modulate the Mucin-Activated Type VI Secretion System of Pandemic *Vibrio cholerae*.
434 PLoS Negl Trop Dis. **2015**; 9(8):e0004031.

435 10. Yoon MY, Min KB, Lee K-M, et al. A single gene of a commensal microbe affects host
436 susceptibility to enteric infection. Nature Communications. **2016**; 7:1–11.

437 11. Mao N, Cubillos-Ruiz A, Cameron DE, Collins JJ. Probiotic strains detect and suppress
438 cholera in mice. Science Translational Medicine. **2018**; 10(445).

439 12. Kaur S, Sharma P, Kalia N, Singh J, Kaur S. Anti-biofilm Properties of the Fecal Probiotic
440 Lactobacilli Against Vibrio spp. Front Cell Infect Microbiol. **2018**; 8.

441 13. You JS, Yong JH, Kim GH, et al. Commensal-derived metabolites govern *Vibrio cholerae*
442 pathogenesis in host intestine. Microbiome.. **2019**; 7(1):1–18.

443 14. David LA, Weil A, Ryan ET, et al. Gut Microbial Succession Follows Acute Secretory
444 Diarrhea in Humans. mBio **2015**; 6(3):e00381–15.

445 15. Midani FS, Weil AA, Chowdhury F, et al. Human Gut Microbiota Predicts Susceptibility
446 to *Vibrio cholerae* Infection. J Infect Dis. **2018**; 218(4):645–653.

447 16. Truong DT, Franzosa EA, Tickle TL, et al. MetaPhlAn2 for enhanced metagenomic
448 taxonomic profiling. Nature Methods. **2015**; 12(10):902–903.

449 17. Franzosa EA, McIver LJ, Rahnavard G, et al. Species-level functional profiling of
450 metagenomes and metatranscriptomes. Nature Methods. **2018**; 15(11):962–968.

451 18. Pasolli E, Truong DT, Malik F, Waldron L, Segata N. Machine Learning Meta-analysis of
452 Large Metagenomic Datasets: Tools and Biological Insights. PLoS Comput Biol. **2016**;
453 12(7):e1004977.

454 19. Fillat MF. The FUR (ferric uptake regulator) superfamily: diversity and versatility of key
455 transcriptional regulators. Arch Biochem Biophys. **2014**; 546:41–52.

456 20. Wang B-Y, Huang H-Q, Li S, et al. Thioredoxin H (TrxH) contributes to adversity
457 adaptation and pathogenicity of *Edwardsiella piscicida*. Vet Res. **2019**; 50(1):1–13.

458 21. Noinaj N, Guillier M, Barnard TJ, Buchanan SK. TonB-dependent transporters: regulation,
459 structure, and function. Annu Rev Microbiol. **2010**; 64:43–60.

460 22. Tett A, Huang KD, Asnicar F, et al. The Prevotella copri Complex Comprises Four
461 Distinct Clades Underrepresented in Westernized Populations. Cell Host and Microbe.
462 **2019**; 26(5):666–679.e7.

463 23. Kovatcheva-Datchary P, Nilsson A, Akrami R, et al. Dietary Fiber-Induced Improvement
464 in Glucose Metabolism Is Associated with Increased Abundance of Prevotella. Cell Metab.
465 **2015**; 22(6):971–982.

466 24. Crost EH, Tailford LE, Le Gall G, Fons M, Henrissat B, Juge N. Utilisation of mucin
467 glycans by the human gut symbiont *Ruminococcus gnavus* is strain-dependent. PLoS ONE.
468 **2013**; 8(10):e76341.

469 25. Tailford LE, Crost EH, Kavanaugh D, Juge N. Mucin glycan foraging in the human gut
470 microbiome. Front Genet. **2015**; 6.

471 26. Sun Y, O'Riordan MXD. Regulation of bacterial pathogenesis by intestinal short-chain
472 Fatty acids. Adv Appl Microbiol. **2013**; 85:93–118.

473 27. Koh A, De Vadder F, Kovatcheva-Datchary P, Bäckhed F. From Dietary Fiber to Host
474 Physiology: Short-Chain Fatty Acids as Key Bacterial Metabolites. Cell. **2016**;
475 165(6):1332–1345.

476 28. Louis P, Flint HJ. Formation of propionate and butyrate by the human colonic microbiota.
477 Environmental Microbiology. **2017**; 19(1):29–41.

478 29. Fachi JL, Souza Felipe J de, Pral LP, et al. Butyrate Protects Mice from *Clostridium*
479 *difficile*-Induced Colitis through an HIF-1-Dependent Mechanism. Cell Reports. **2019**. p.
480 750–761.e7.

481 30. Fukuda S, Toh H, Hase K, et al. Bifidobacteria can protect from enteropathogenic
482 infection through production of acetate. Nature. **2011**; 469(7331):543–547.

483 31. Canani RB, Costanzo MD, Leone L, Pedata M, Meli R, Calignano A. Potential beneficial
484 effects of butyrate in intestinal and extraintestinal diseases. World J Gastroenterol. **2011**;
485 17(12):1519–1528.

486 32. Yang W, Xiao Y, Huang X, et al. Microbiota Metabolite Short-Chain Fatty Acids
487 Facilitate Mucosal Adjuvant Activity of Cholera Toxin through GPR43. The Journal of
488 Immunology. **2019**; 203(1):282–292.

489 33. Rabbani GH, Albert MJ, Rahman H, Chowdhury AK. Short-Chain Fatty Acids Inhibit
490 Fluid and Electrolyte Loss Induced by Cholera Toxin in Proximal Colon of Rabbit In
491 Vivo. Dig Dis Sci. **1999** 44(8):1547–1553.

492 34. Sepúlveda Cisternas I, Salazar JC, García-Angulo VA. Overview on the Bacterial Iron-
493 Riboflavin Metabolic Axis. Front Microbiol. **2018**; 9:1478.

494 35. Rivera-Chávez F, Mekalanos JJ. Cholera toxin promotes pathogen acquisition of host-
495 derived nutrients. Nature. **2019**; 572(7768):244–248.

496 36. Sepúlveda Cisternas I, Aguirre LL, Flores AF, de Ovando IVS, García-Angulo VA.
497 Transcriptomics reveals a cross-modulatory effect between riboflavin and iron and outlines
498 responses to riboflavin biosynthesis and uptake in *Vibrio cholerae*. Scientific Reports.
499 **2018**; 8(1):1–14.

500 37. Schmidt TSB, Raes J, Bork P. The Human Gut Microbiome: From Association to
501 Modulation. Cell. **2018**; 172(6):1198–1215.

502